

Two distinctive binding modes of endonuclease inhibitors to the N-terminal region of influenza virus polymerase acidic subunit

Tyuji Hoshino^{1,*}, Satoshi Fudo¹, Yuji Komukai¹ and Michiyoshi Nukaga²

¹ Graduate School of Pharmaceutical Sciences, Chiba University,
1-8-1 Inohana, Chuo-ku, Chiba 260-8675, Japan

² Faculty of Pharmaceutical Sciences, Josai International University,
Gumyo 1, Togane-shi Chiba 283-8555, Japan

1 Introduction

Endonuclease activity of influenza virus is one of the potential targets for antiviral drugs since the activity is vital for the viral life cycle. So far, several classes of compounds have been identified as the endonuclease inhibitors of influenza viruses.

In our previous study, we performed an *in vitro* chemical screening and identified three compounds which blocked the function of PA_N.¹ Additionally, we elucidated the complex structure of PA_N with one of the inhibitory compounds by X-ray crystal structure analysis. In this study, we clarified the two crystal structures of PA_N with the other two inhibitory compounds. To our surprise, the binding modes of the two inhibitory compounds to PA_N were different from a common binding mode previously reported for many other influenza virus endonuclease inhibitors. Therefore, we additionally clarified the crystal structure of PA_N with each inhibitory compound at pH 7.0 to examine whether the binding modes of the two compounds were affected by the crystallization condition. Furthermore, we performed molecular dynamics (MD) simulations based on the respective crystal structures at pH 7.0 in order to understand how those inhibitory molecules interacted with PA_N and to evaluate the stability of the binding poses. Lastly, we carried out a crystal structure analysis and an MD simulation for PA_N with another inhibitor, which was already reported to have a high compound potency to compare the stability of the binding mode.

2 Experiment

Truncated PA_N protein, PA_N^{Δloop}, from A/Puerto Rico/8/34 (PR8) strain (H1N1) was expressed and purified. The *Escherichia coli* strain Rosetta (DE3) pLysS transformed with the pET50b(+) vector containing the PA_N^{Δloop} gene was cultured in LB medium. The protein was expressed at 17 °C for 48 hours after induction at an OD₆₀₀ value of 0.8-1.0 with 0.2 mM IPTG. The protein was purified by a HisTrap HP column (GE Healthcare), followed by the cleavage of 6×His-fused Nus-tag by HRV 3C protease. The cleaved protein was again purified by Ni-NTA resin (Novagen) and TALON resin (Clontech). The protein was further purified by gel filtration using HiLoad 16/60 Superdex 200 pg (GE Healthcare) with a running buffer of 20 mM Tris-HCl at

pH 8.0 and 100 mM NaCl. Finally, the protein was concentrated to 9.9 mg/mL.

Crystals of PA_N^{Δloop} were grown by the vapor diffusion method with hanging drops consisting of 1.0 μL of 9.9 mg/mL protein solution containing 4.0 mM MnCl₂ and 1.0 μL of well solution (100 mM MES at pH 5.8, 1.1 M ammonium sulfate, 0.1 M potassium chloride and 9% (v/v) trehalose) at 18°C. In order to obtain complex structures with inhibitors (PA_N-compound **1**, and PA_N-compound **2**), crystals were soaked with the well solution containing 10.0 mM MnCl₂ and 4.0 mM each inhibitory compound for 2.0 hours. To obtain complex structures with inhibitors at pH 7.0 (PA_N-compound **1** at pH7.0, PA_N-compound **2** at pH7.0, and PA_N-compound **3** at pH7.0), pH of the well solution was change to 7.0, and crystals were soaked in the same manner. The crystals were then cryo-protected by brief immersion in well solution containing 22.5% (v/v) glycerol, followed by flash-freezing in liquid nitrogen.

The X-ray crystal structures obtained at pH 7.0 in this work were used as the initial structures for MD simulation. For the calculation models, the crystal structures were modified by replacing two manganese ions at the active site with two magnesium ions since magnesium ions are probably more biologically relevant cofactors for endonuclease activity of PA_N and by replacing sulfate ion with chloride ion.

A general AMBER force field (GAFF) was applied to each inhibitory compound and ff10 force field was to the other molecules. Each model complex was placed in a rectangular box filled with TIP3P water molecules using the LEaP module. Counter ions were added to neutralize each model system. Energy minimization, heating, and MD simulations were performed with the pmemd module in AMBER 14. First, energy minimization only for water molecules and counter ions were performed. Second, energy minimization was executed again with all the atoms except those of the inhibitory compound and magnesium ions being set free. Energy minimizations were performed by the steepest descent method for the first 3,000 cycles and by the conjugated gradient method for the subsequent 7,000 cycles. Then the calculation system was heated to 310 K for 0.1 ns under the NVT-ensemble condition. Third, all of the atoms were again minimized and then the system was heated to 310 K for 0.1 ns under the NVT-ensemble condition. After the

heating, pre-equilibrated calculation was performed for 0.4 ns under the NPT-ensemble condition. Then, the production run of MD simulation was carried out for 100 ns with an integration time step of 2.0 fs under the NPT-ensemble condition (1 atm, 310 K). The cutoff distance for the long-range interaction terms was set to 12.0 Å. The expansion and shrinkage of all the covalent bonds involving hydrogen atom are constrained by the SHAKE algorithm. Periodic boundary condition was applied to avoid the edge effect.

3 Results and Discussion

We already identified three compounds which blocked PA_N endonuclease activity through an *in vitro* chemical screening and measured the potency of those compounds.¹ The crystal structure of truncated PA_N ($PA_N^{\Delta loop}$) in complex with one of the compounds was already reported. In the present study, we firstly clarified complex structures of $PA_N^{\Delta loop}$ with the other two compounds, obtained by soaking at pH 5.8 (PA_N -compound **1** at pH 5.8 and PA_N -compound **2** at pH 5.8) and apo form of $PA_N^{\Delta loop}$ (PA_N -apo). Secondly, we clarified complex structures of $PA_N^{\Delta loop}$ with compounds **1**, **2**, and **3**, obtained by soaking at pH 7.0 (PA_N -compound **1** at pH 7.0, PA_N -compound **2** at pH 7.0, and PA_N -compound **3** at pH 7.0). The results of the crystal analysis at pH 5.8 are described first. Crystal structures of PA_N -apo, PA_N -compound **1** at pH 5.8, and PA_N -compound **2** at pH 5.8 were found to be in the same space group (Table 1). Sizes of crystal lattice were almost same among those crystal structures although that of PA_N -compound **1** was slightly larger.

In order to examine whether the binding modes of the two inhibitors obtained in Table 1 were affected by the soaking condition, we clarified the crystal structure of PA_N with each inhibitory compound at neutral pH. The co-crystals in Table 1 were obtained at pH 5.8, which was the same as the well solution for protein crystallization. In contrast, the co-crystallization was performed at pH 7.0 by changing pH of the well solution to 7.0 only in the soaking step (Table 2, PA_N -compound **1** at pH 7.0 and PA_N -compound **2** at pH 7.0). In the crystal structures at pH 7.0, one, two, and one molecules were observed for compounds **1**, **2**, and **3**, respectively. Hence, they were denoted as molecule **1A'**, molecule **2A'**, molecule **2B'**, and molecule **3** for clarity. The crystal structure of PA_N -compound **3** at pH 7.0 will be mentioned later. In the crystal structure of PA_N -compound **1** at pH 7.0, molecule **1A'** was bound to the active site in the almost same way as molecule **1A**. A molecule corresponding to molecule **1B** was not observed. Although there was a difference in that a water molecule was observed at the M1 site in the crystal structure at pH 7.0, a manganese ion was not coordinated to the M1 site even at pH 7.0. Therefore, compound **1** can expel a metal ion from the M1 site even at physiological condition. A possible explanation for the existence of a water molecule in the M1 site is that the protonation state of the side chain of His41 was changed between the structures at pH 5.8 and 7.0 since pKa of the side chain of histidine is usually 6.0 (Fig. 1a).

Table 1: Crystallographic data collection, refinement statistics, and chemical structures of inhibitory compounds for PA_N -apo, PA_N -compound **1** at pH 5.8, and PA_N -compound **2** at pH 5.8.

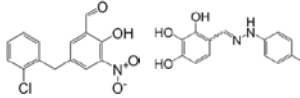
	PA_N -apo	PA_N - compound 1 at pH 5.8	PA_N - compound 2 at pH 5.8
Data collection			
X-ray source	AR-NE3A, PF, KEK	BL5A, PF, KEK	BL5A, PF, KEK
Wavelength (Å)	1.000	1.000	1.000
Space group	$P4_12_12$	$P4_12_12$	$P4_12_12$
<i>a, b, c</i> (Å)	66.33, 66.33, 127.34	66.56, 66.56, 129.17	66.76, 66.76, 126.74
Total no. reflections	423428	126278	374092
Unique no. reflections	30558	10200	27032
Resolution (last shell) (Å)	50.00-1.70 (1.73-1.70)	50.00-2.50 (2.54-2.50)	50.00-1.80 (1.83-1.80)
Completeness (last shell) (%)	95.1 (99.4)	95.6 (93.3)	98.8 (100.0)
R_{merge} (last shell)	0.072 (0.900)	0.136 (0.000)	0.060 (0.000)
$I/\sigma I$ (last shell)	28.584 (3.465)	16.255 (2.583)	36.194 (2.500)
Redundancy (last shell)	13.9 (14.4)	12.4 (12.8)	13.8 (14.2)
Sigma cut-off (<i>I</i>)	$ I < -3.0\sigma$	$ I < -3.0\sigma$	$ I < -3.0\sigma$
Refinement			
Resolution (Å)	29.41-1.80	38.04-2.50	32.28-1.80
No. reflections (R_{free} set)	25617 (1316)	10153 (472)	26966 (1354)
R_{work}/R_{free}	0.224/0.274	0.222/0.270	0.200/0.225
No. atoms/Mean <i>B</i> -factors(Å ²)			
all	1737/36.35	1612/42.69	1722/44.67
protein	1493/34.32	1493/40.69	1493/43.04
inhibitor	0/0.00	40/65.75	19/53.26
water	237/48.47	73/43.86	203/55.15
other	7/59.26	6/104.40	7/65.33
Ramachandran (%)			
Favored	98.9	99.4	98.3
Outliers	0.0	0.0	0.0
RMS bond (Å)	0.010	0.004	0.013
RMS angle (°)	1.23	0.79	1.44
Compound Structure			

Table 2: Crystallographic data collection, refinement statistics, and chemical structures of inhibitory compounds for PAN-compound **1** at pH 7.0, PAN-compound **2** at pH 7.0, and PAN-compound **3** at pH 7.0.

	PAN-compound 1 at pH 7.0	PAN-compound 2 at pH 7.0	PAN-compound 3 at pH 7.0
Data collection			
X-ray source	BL17A, PF, KEK	BL17A, PF, KEK	BL17A, PF, KEK
Wavelength (Å)	0.980	0.980	0.980
Space group	<i>P</i> 4 ₁ 2 ₁ 2	<i>P</i> 4 ₁ 2 ₁ 2	<i>P</i> 4 ₁ 2 ₁ 2
<i>a</i> , <i>b</i> , <i>c</i> (Å)	66.40, 66.40, 127.39	66.58, 66.58, 128.31	66.44, 66.44, 126.98
Total no. reflections	117975	145354	210260
Unique no. reflections	10401	16066	17513
Resolution (last shell) (Å)	50.00-2.50 (2.54-2.50)	50.00-2.15 (2.19-2.15)	50.00-2.10 (2.14-2.10)
Completeness (last shell) (%)	99.9 (100.0)	98.0 (99.4)	99.2 (98.7)
<i>R</i> _{merge} (last shell)	0.152 (1.195)	0.074 (1.034)	0.115 (1.100)
<i>I</i> / <i>σ</i> (last shell)	18.628 (3.625)	25.351 (2.320)	22.150 (2.676)
Redundancy (last shell)	11.3 (8.8)	9.0 (9.0)	12.0 (11.3)
Sigma cut-off (<i>I</i>)	<i>I</i> < -3.0 σ	<i>I</i> < -3.0 σ	<i>I</i> < -3.0 σ
Refinement			
Resolution (Å)	46.96-2.50	44.20-2.15	46.98-2.10
No. reflections (<i>R</i> _{free} set)	10354 (550)	16051 (813)	17480 (915)
<i>R</i> _{work} / <i>R</i> _{free}	0.201/0.232	0.205/0.227	0.190/0.228
No. atoms/Mean <i>B</i> -factors(Å ²)			
all	1542/59.34	1568/48.36	1628/37.35
protein	1493/58.76	1493/47.71	1493/36.72
inhibitor	20/93.08	38/74.19	29/45.49
water	23/54.75	30/43.94	99/42.82
other	6/108.06	7/66.12	7/60.28
Ramachandran (%)			
Favoured	98.3	98.9	98.3
Outliers	0.0	0.0	0.0
RMS bond (Å)	0.006	0.009	0.008
RMS angle (°)	0.79	1.08	1.71
Compound Structure			

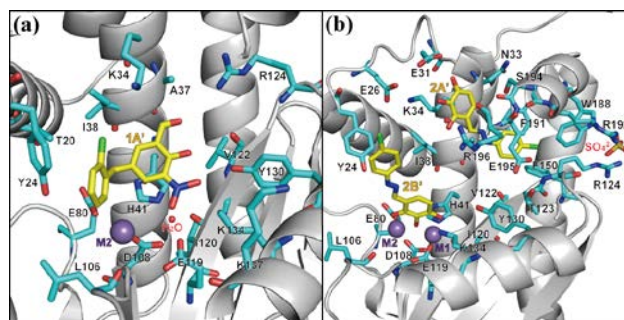


Fig. 1: Crystal structure of PAN-compound **1** at pH 7.0 (a) and PAN-compound **2** at pH 7.0 (b). Protein backbone is depicted in cartoon (gray), manganese ions are in sphere (magenta), and inhibitory molecules are in the stick representation colored yellow (carbon), red (oxygen), blue (nitrogen), and green (chlorine). The residues near the inhibitory molecules are shown in the stick representation colored cyan (carbon), red (oxygen), and blue (nitrogen) with the labels of their residue names.

Since the difference in structure between pH 5.8 and 7.0 was slight, the crystal structure at pH 7.0 supported the essence of the unique binding mode of compound **1** to PAN.

A more remarkable difference was seen for the binding mode of compound **2** between the crystal structures at pH 5.8 and pH 7.0 (Fig. 1b). In the crystal structure of PAN-compound **2** at pH 7.0, there were two molecules of compound **2**, molecules **2A'** and **2B'**. The binding mode of molecule **2A'** is similar to that of molecule **2A**. Molecule **2B'**, which was additionally observed only at pH 7.0, made a chelation to the two manganese ions in the active site by its trihydroxyphenyl group. This binding mode is acceptable because many other PAN endonuclease inhibitors were reported to chelate to the metal ions in the active site by their metal-chelation motifs. As a result, it seems reasonable to consider that the crystal structure at pH 5.8 was influenced by the protonation states of the inhibitory compound and the protein. Nevertheless, similar binding modes of molecules **2A** and **2A'** suggest that compound **2** can be utilized as an anchor fragment to fasten inhibitors to PAN.

MD simulations were performed for the crystal structure of PAN-compound **1** at pH 7.0 and that of PAN-compound **2** at pH 7.0. In both of the PAN-compound **1** and **2** complex models, RMSD values for main chain atoms of the protein from the initial structure remained below 3.0 Å during the 100-ns simulation. Major conformational changes and/or positional changes of compound **2** during the simulations were depicted in Fig. 2. During the 100-ns simulation with compound **2**, the conformation and the position of molecule **2A'** were almost unchanged (Figures 6a-6h). This means the molecule was stably bound to the site in the almost same binding pose as that of the crystal structure. The trihydroxyphenyl moiety of molecule **2B'** also stably maintained interactions with the two metal ions in the active site during the simulation. On the other hand, the *p*-chlorophenyl group of molecule **2B'** continued to

fluctuate to a small extent, which suggested this moiety was not capable of making strong interaction with protein residues. Nevertheless, the position and conformation of molecule **2B'** were almost maintained during the simulation. No obvious direct interaction was observed between molecules **2A'** and **2B'** in the simulation.

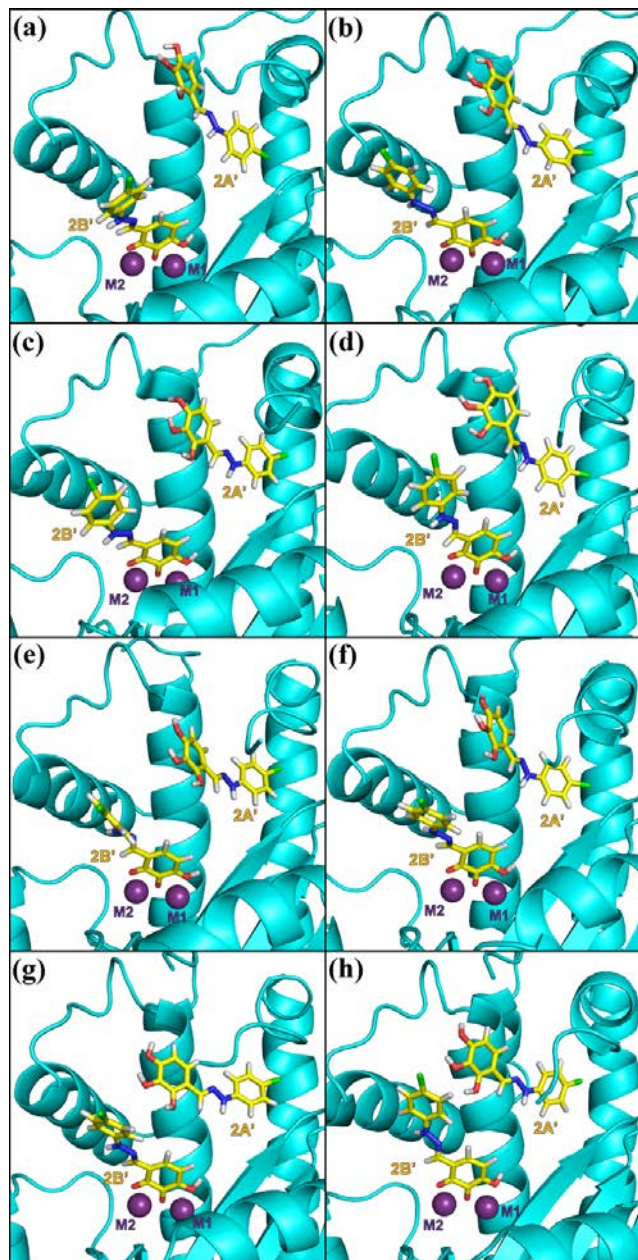


Fig. 2: Eight extracted structures from the 100-ns MD simulation with compound **2**. Structures at 1 ns (a), 5 ns (b), 10 ns (c), 20 ns (d), 40 ns (e), 60 ns (f), 80 ns (g), and 100 ns (h) are displayed. Protein backbone is depicted in cartoon (cyan), magnesium ions are in spheres (magenta), and molecules **2A'** and **2B'** are in the sticks colored yellow (carbon), red (oxygen), blue (nitrogen), and green (chlorine).

In conclusion, Crystal structures of PA_N^{Aloop} with two endonuclease inhibitors clarified unique binding modes of these inhibitors. In the crystal structure of PA_N -compound

1 at pH 5.8, one of the metal binding sites (M1 site) was buried by the nitro group of molecule **1A**. In the crystal structure of PA_N -compound **2** at pH 5.8, molecule **2A** was not bound to metal ions in the active site. Instead, the compound molecule was positioned apart from the metal ions and inserted into the hydrophobic space caused by the flip of the side chain of Arg124. Additional X-ray crystal structure analysis was performed to examine the influence of pH condition in the soaking step on the binding mode of compounds in the crystal structures. The crystal structure of PA_N -compound **2** at pH 7.0 contained two molecules of compound **2** at the active site, one of which showed a binding mode almost identical to that obtained at pH 5.8, and the other of which chelated to the two metal ions. Furthermore, 100-ns MD simulations based on the crystal structures at pH 7.0 revealed the stability of the inhibitor molecules. These binding modes were examined in detail in terms of B-factor values, binding free energy, and deviation from the crystal structures. The crystal structure and the following MD simulation of PA_N -compound **3** at pH 7.0 showed a different binding mode from that in the previous report and compound **3** partly changed its conformation in the MD simulation from the crystal structure. These findings demonstrate that the binding poses of inhibitors are affected by the pH conditions and the compound conformation sometimes fluctuates through MD simulation. The structural information obtained in this work will be useful for further development of novel potent endonuclease inhibitors.

Acknowledgement

Calculations were performed at Research Center for Computational Science, Okazaki, Japan and at Information Technology Center of the University of Tokyo. This work has been performed under the approval of the Photon Factory Program Advisory Committee (proposal no. 2012G658, 2014G563).

References

- [1] S. Fudo *et al.*, *Bioorg. Med. Chem.* **23**, 5466 (2015).
- [2] S. Fudo *et al.*, *Biochemistry* **55**, 2646 (2016).

* hoshino@chiba-u.jp